EVERGLASS

EVERGLASS: The new role of glass in a sustainable society

WP2: Conditioning of glass wastes and convert into glass powder

Publish Date: 20-09-2024

Author: Dr. María Jesús Pascual

Funded by the European Union

Technical References

Project Acronym	EverGLASS
Project Title	The New Role of Glass in a Sustainable Society. Technology for the Integral Recycling of Glass
Project Coordinators	Juan Pou / Rafael Comesaña
Project Duration	36 months

Deliverable No.	2.1
Dissemination level [1]	PU
Work Package	Conditioning of glass wastes and convert into glass powder
Task	Task 2.1: Study on the glass waste heterogeneity factors Task 2.2: Compositional characterisation of different types of glass waste Task 2.3: Thermal characterisation Task 2.4: Milling and sieving of the precursor material and optimization of the particle size.
Lead beneficiary	ICV- CSIC
Contributing beneficiary(ies)	ICV-CSIC, TNUAD/FunGlasS
Due date of deliverable	30-09-2024
Actual submission date	20-09-2024

1 PU = Public
PP = Restricted to other programme participants (including the Commission Services)
RE = Restricted to a group specified by the consortium (including the Commission Services)
CO = Confidential, only for members of the consortium (including the Commission Services)

Document history

V	Date	Beneficiary	Author
V0.1	20/ 09/ 2024	ICV-CSIC	María Jesús Pascual
V0.2			
V0.3			
V1			

Summary

Summary of Deliverable

This research provides a comprehensive analysis of various types of glass materials, both commercial glasses and recycled wastes, with a focus on their chemical and physico-chemical properties. The first stage was the stockpiling of materials and its classification by procedence and glass composition system. The study of the collected glasses included a detailed characterisation using several advanced techniques, such as chemical analysis with X-ray fluorescence, measurement of thermal expansion coefficient by dilatometry, and viscosity determination by hot-stage microscopy, among others. The primary objective is to understand the thermal properties, in particular the viscosity-temperature behaviour of the glasses in order to define the operational conditions for further laser melting.

The analysis reveals significant differences in the properties of commercial glasses, such as borosilicate glass Duran®, soda-lime window glass, and borosilicate glass Covid vaccine vials, with particular emphasis on their thermal expansion coefficients and viscosity-temperature relationships. The results highlight how variations in chemical composition, such as the presence of Al_2O_3, B_2O_3 and alkali oxides, affect the viscosity and thermal stability of the glass.

Recycled glasses, including those from household containers and a waste management company, were also analysed, showing similar compositions across different types of soda-lime glass, but with minor differences attributable to their specific uses and sources. These glasses were first cleaned to remove any contaminants (label and other possible residues) and then ground to obtain an optimal particle size for further processing in the laser morphing machine, which was 100-300 µm.

The document concludes that understanding these properties is crucial for optimising the recycling and reuse of glass materials in sustainable applications, aligning with the broader goal of the project to promote sustainability in the glass industry.

Disclaimer

Funded by the European Union. Views and opinions expressed are however those of the author(s) only and do not necessarily reflect those of the European Union or European Commission. Neither the European Union nor the granting authority can be held responsible for them.

Table of contents

Table of tables

Table of figures

1 Stockpiling of materials

This section presents the different glass materials that have been collected. Two types of materials can be distinguished: commercial glass with certified composition and recycled glass. Commercial glasses have been selected whose composition is certified and highly homogeneous. The main reason for using glasses with these characteristics is that their properties, especially their thermal properties, are well known, making them ideal reference candidates to study the melting behavior by means of the Glass Laser Morphing (GLM).

The materials selected were:

- Silica glass (SiO_2, www.vidrasa.com)
- Borosilicate glass (Duran®, Pyrex®)
- Sodalime glass (Flat glass, window glass from Saint- Gobain, Avilés, Spain)
- Pharmaceutical glass (borosilicate and aluminosilicate systems)

The pharmaceutical glass has been obtained from the recycling of vaccine vials. On one hand, covid vaccine vials have been collected after use from a health center in Madrid. On the other hand, vials from Nuova Ompi (Stevanato group) have been provided by TNUAD. This glass will be referred to as pharmaceutical glass waste (PGW).

On the other hand, the collection of recycled glass comprises:

- Containers (jars, wine bottles, beer bottles, olive oil bottles, etc.) collected from home, bars and restaurants. These are sodalime glasses of different colours (white, different greens, ambar, blue).
- External cullet- glass waste management company in Barcelona (https://danielrosas.com/). These wastes are mainly containers of sodalime glass (white and mixed colours) and also float glass (window glass).
- Glass- ceramics from cooktop panels (provided by Copreci group from Mondragon group, Basque country).
- Borosilicate glass (Pyrex) from material lab wastes.
- Monitors, screens, isolation and reinforcement fibers, and others.

The characterization of these materials is being carried out at the ICV-CSIC. The following techniques and methods are being used:

- Chemical analysis (X-ray fluorescence). Boron was analyzed by ICP- Oes.
- Density and physico- chemical properties (Dilatometry, Young modulus, etc.) and technical specifications.
- Determination of the viscosity- temperature curve using Hot- stage microscopy (HSM) and high temperature viscometer.
- Milling and sieving (100- 300 µm ideally, maximum 800 µm). Particle size determination by laser diffraction (Mastersizer S, Malvern).
- UV spectra of polished glass pieces with 2 mm of thickness.
- Melting of wastes in electrical and gas furnaces.

1.1 Characterisation of the commercial glasses

1.1.1 Chemical analysis

Table 1 presents the chemical analysis, both in wt.% and mol% for Duran® glass, window glass (sodalime glass from Saint Gobain, Avilés), covid vaccine vials and pharmaceutical glass waste. The results obtained are very similar to those given by the supplier companies providing Duran® and window glasses. On the other hand, the glass from the covid vaccine vials has a composition typical of borosilicate glasses type I and III used for pharmaceutical purposes [1].The chemical analysis was repeated in TNUAD with a very similar result.

Table 1 Chemical analysis of commercial glasses.

Components	Duran® Glass		Window glass		Covid vaccine vials		PGW	
	wt.%	mol%	wt.%	mol%	wt.%	mol%	wt.%	mol%
SiO_2	82.10	84.71	73.20	72.50	76.30	79.31	72.40	76.35
B_2O_3	11.00	9.80			9.50	8.52	10.9	9.92
Al_2O_3	2.47	1.50	0.80	0.47	5.30	3.25	6.9	4.29
Na_2O	3.63	6.63	13.40	12.87	7.20	7.26	6.7	6.85
K_2O	0.55	0.36	0.27	0.17			1.5	1.01
CaO			9.50	10.08	1.41	1.57	1.3	1.46
MgO			2.50	3.69			0.05	0.08
SO_3			0.22	0.16			0.003	0.002
Fe_2O_3			0.06	0.02	0.06	0.02	0.01	0.004
TiO_2			0.05	0.04	0.03	0.02	0.04	0.03
ZrO_2					0.07	0.04		
As_2O_3					0.045	0.01		

In the case of Duran® glass, we also have a series of physical data given by the company which are listed in Table 2.

Table 2 Physical data provided by the supplier company.

Duran® Glass	
Density (ρ) at 25 °C	2.23 $g \cdot cm^{-3}$
Average thermal expansion coefficient α (20 °C; 300 °C)	$3{,}3.10^{-6}$ K^{-1} according to ISO 7991
Glass transition temperature (T_g):	525 °C
Glass temperatures for the viscosities η in dPa.s	
10^{13} superior annealing temperature	560 °C
$10^{7,6}$ softening temperature	825 °C
10^4 working temperature	1260 °C

1.1.2 Dilatometry

In order to obtain the values of thermal expansion coefficient (α), glass transition temperature (T_g) and dilatometric softening temperature (T_d), dilatometric measurements were carried out on the Netzsch Gerätebau Differential Dilatometer Model 402 EP.

Figure 1 shows the dilatometric curves for Duran® and window glass. The T_g obtained was 525 ± 2 °C and 550 ± 2 °C, respectively, while the thermal expansion coefficient, calculated for the range 100- 500 °C, was 3.4 ± 0.5 $\cdot 10^{-6}$ K^{-1} for the Duran® and 9 ± 0.5 $\cdot 10^{-6}$ K^{-1} for the window glass. Finally, the T_d was 598 °C and 602 °C, respectively. As it can be seen, the difference in thermal properties is remarkable, especially the coefficient of thermal expansion, this has a direct impact on the laser processing conditions. Additionally, in principle the borosilicate glass with lower thermal expansion coefficient will be more resistant versus thermal shock and so it will show less tendency to cracks formation after cooling. As observed by the chemical analysis study, window glass has a higher alkali content, which increases the value of the coefficient of expansion.

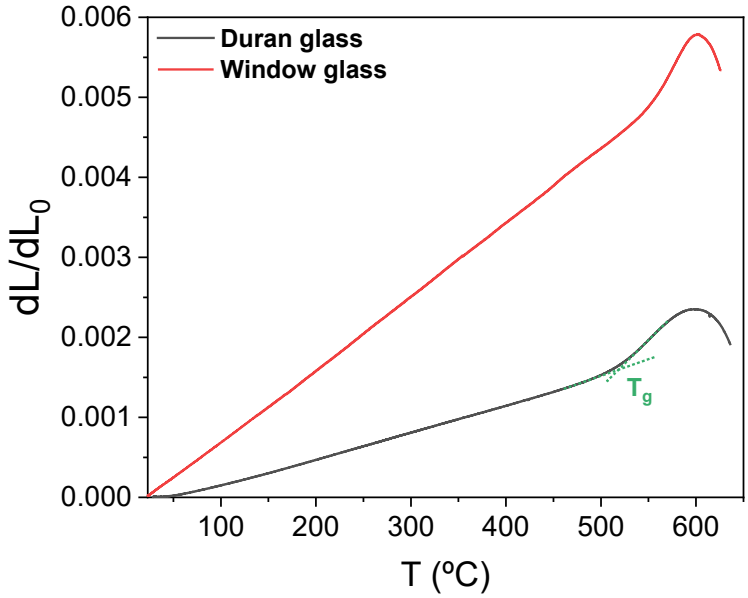

Figure 1 Dilatometric curves for Duran® and window glasses.

The same study was carried out for the PGW sample using TMA Q400 equipment in TNUAD. The T_g was 567 °C, T_d was 697 °C.and the thermal expansion coefficient calculated at 300, 4.9 $\cdot 10^{-6}$ K^{-1}.

1.1.3 Hot- stage microscopy (HSM)

HSM curves have been studied for the three glasses: Duran®, window and Covid® vaccine vials (Figure 2). From the results obtained by this technique, information on the viscosity fixed points can be extracted. The graph shows two temperatures, the temperature of first sintering (T_{FS}) and the temperature of maximum sintering (T_{MS}). Table 3 shows the results obtained for the three glasses with particle size bellow 20 µm.

Table 3 Temperatures of fixed viscosity points.

	TFS ± 10°C ($10^{9.1}$ dPa·s)	TMS ± 10°C ($10^{7.8}$ dPa·s)	Softening point ± 10 °C ($10^{6.3}$ dPa·s)	Sphere ± 10 °C ($10^{5.4}$ dPa·s)	Half- ball ± 10 °C ($10^{4.1}$ dPa·s)	Fluence ± 10 °C ($10^{3.4}$ dPa·s)
Duran®	689	801	870	1140	1235	1431
Window glass	628	709	793	849	979	1142
Covid® vaccine vials	675	760	874	910	1129	1427

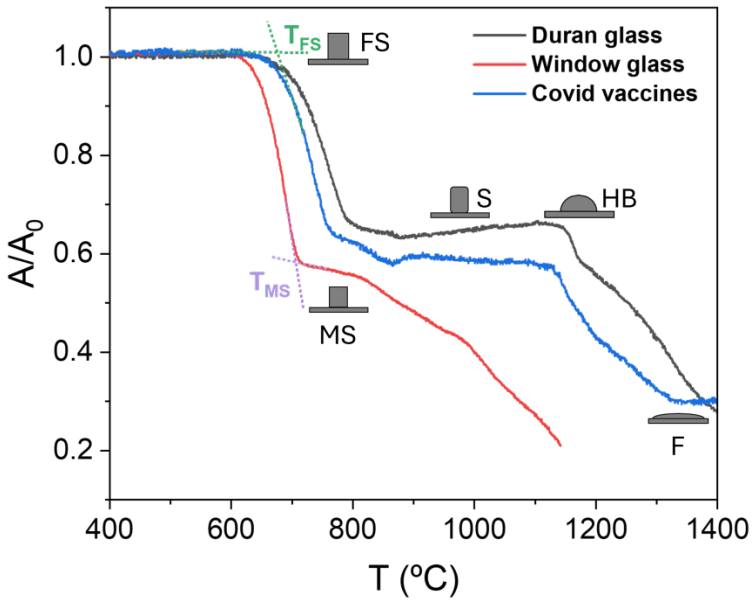

Figure 2 Hot- stage microscopy curves for commercial glasses.

Table 4 shows the fitting parameters obtained from the Vogel - Fulcher - Tammam equation (VTF, eq. 1), where viscosity versus temperature is plotted. T_g data have been included which corresponds to log(η) = 13.3 dPa·s. Likewise, for Duran® and window glass (Annex 1), the data provided by the commercial companies have been included. Figure 4 shows the viscosity-temperature curves for Duran® and Covid vaccine vials and window glass.

$$log\,\eta = A + \frac{B}{T - T_0} \qquad \text{Eq. 1}$$

From the fit, the parameters A, B, and T_0 of the equation can be obtained. For these three glasses the viscosity increases in the following order: Window glass<Covid® vaccine vials< Duran® glass (Figure 3). The behaviour of these glasses at low temperatures can be explained by the Al_2O_3 content of these glasses. The Al_2O_3 in the glassy lattice is in tetrahedral configuration [AlO_4] and alternates with the [SiO_4] groups, so that the number of non-bridging oxygens decreases causing the viscosity to increase, especially at low temperatures.

These glasses have alkaline and alkaline earth oxides in their composition. The higher the field strength, the greater the bonding energy of modifier ions to the bridging oxygens, weakening the structure. MgO causes a decrease in viscosity at high temperatures, in the same way as CaO, although CaO causes it to increase at low temperatures. On the other hand, Na_2O lowers the viscosity over the whole temperature range.

Table 4 VFT parameters of the viscosity-temperature curves.

VFT parameters	A	B	T_0
Duran® glass	-0.278	4689.8	204.7
Window glass	-2.074	4922.8	201.0
Covid® vaccine vials	0.359	3207.5	313.0

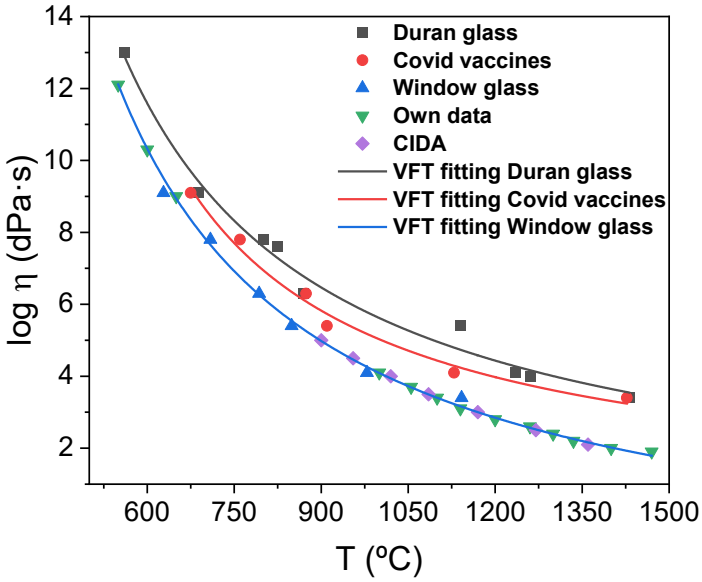

Figure 3 Viscosity-temperature curves for a) Duran glass and Covid vaccine vials (borosilicate glasses) and b) window glass (sodalime glass, float glass).

Finally, the viscosity of PGW glass has been estimated using the tool provided by https://glassproperties.com/. Annex 2 shows the estimated viscosity and temperature data for PGW glass.

Figure 4 shows the viscosity-temperature curves for PGW in powder and microspheres, while Table 5 shows A, B and T_0 parameters obtained from VFT equation (Eq. 1). In this case, although the composition in both cases is practically the same, the viscosity for microsphere glass has a higher viscosity than powdered glass because of the volatilization of alkaline components during the sphere fabrication process These spheres will be used as reference material to study the interaction with the laser in totally spherical particles.

Table 5 Parameters for fitting the equations of the viscosity-temperature curves.

Parameters	A	B	T_0
PGW glass powder	-2.021	5801.2	182.1
PGW glass microsphere	-2.236	6708.5	154.5

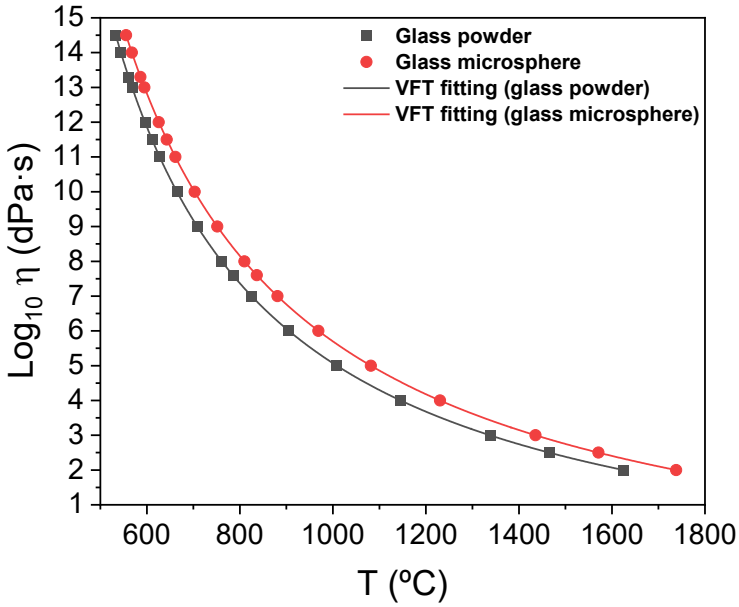

Figure 4 Viscosity-temperature curves for PGW in glass powder and glass microspheres.

1.1.4 Particle size

For the GLM process, milled glass with an optimum particle size between 100- 300 µm (maximum size 800 µm) has to be conditioned. Particle size determination after milling has been performed for Duran® glass and Covid® vaccine vials (Figure 5). For both glasses, the particle size is below 400 µm with an average size around 200 µm.

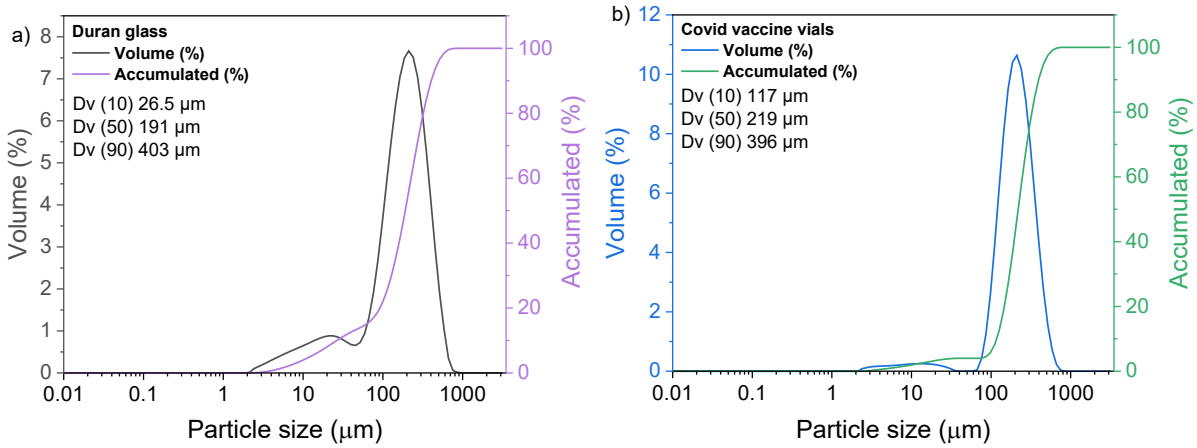

Figure 5 Particle size distribution of glass powder Duran® and Covid® vaccine vials.

On the other hand, for PGW glass, 3 batches with different particle sizes were prepared (Table 6). The first two batches were prepared by fusion and the third batch was prepared by flame synthesis (FS).

Table 6 PGW-prepared batches with different particle sizes.

Glass system/ batch	Batch-1 (120 g)	Batch-2 (120 g)	Batch-3 for FS (120 g)
Pharmaceutical glass (PGW)	<125 (µm)	125- 315 (µm)	<125 (µm)

The particle size has been measured for all three batches by SEM. Figure 6 shows both the surface area of the samples and the size distribution. For Batch-1 a mean particle size around 52 µm with a maximum size of 128 µm is observed (Figure 7a)). For Batch-2, on the other hand, the mean size is around 220 µm with a mean size of 376 µm (Figure 7b)). Finally, Batch-3 has a mean size of 48 µm and a maximum size of 129 µm (Figure 7c)). Also, if we look at the surface of the batches, the first two batches are similar showing the typical fractured surfaces of grinded glass while the third one are microspheres with polished surfaces.

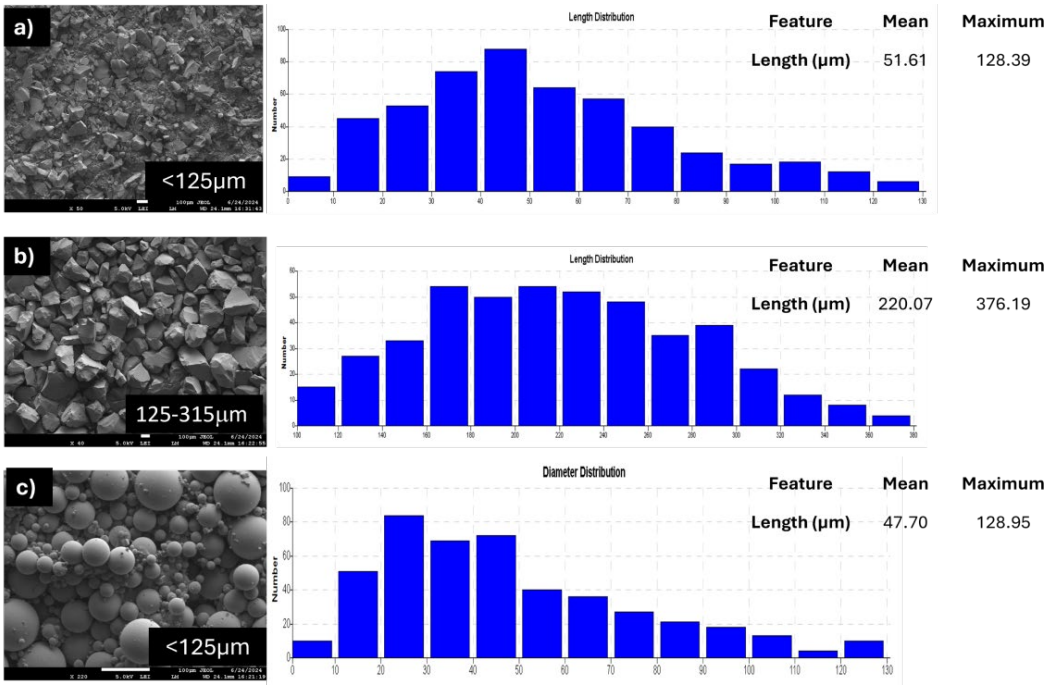

Figure 6 Particle size distribution for a) Batch-1, b) Batch-2 and c) Batch-3.

1.2 Characterisation of the recycling glass

In this section, the characterisation results for recycled glass are presented. These different coloured glasses (white, different greens, amber, blue) are mainly containers (jars, wine bottles, beer bottles, olive oil bottles, etc.) collected from households, bars or restaurants (Figure 7).

Figure 7 Picture of the containers, from left to right: white container, wine bottle (green), beer bottle (green and amber), and water bottle (blue).

This section also includes the characterisation results obtained for the glass from the recycling company (white, microflat and mixed glass) (Figure 8).

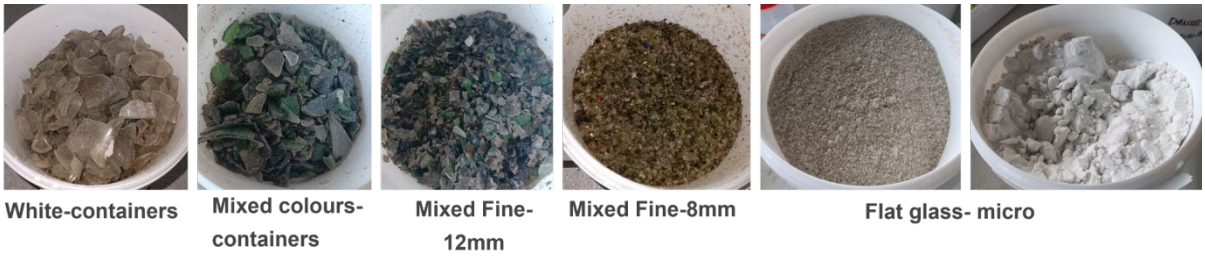

Figure 8 Picture of the glasses from the recycling company.

1.2.1 Chemical analysis

Table 7 presents the chemical analysis, both in wt.% and mol% studied for the glass recycling (containers and glasses from the recycling company). As it can be seen, the container glasses have a very similar composition, they are all sodalime glasses and present small differences in certain elements that give them their characteristic colour. On the other hand, it can be observed that the composition of the laboratory glass (Table 7) and the commercial Duran glass (Table 1) is very similar (both are borosilicate glasses), although in the laboratory glass there are also other types of alkaline oxides (MgO or CaO), and other oxides (such as TiO_2 or SO_3) which are not observed in the composition of the Duran glass.

On the other hand, Table 8 presents the results obtained for the glass from the recycling company. As before, the compositions are very similar to each other and compared to those obtained for the container glasses they are also very similar. This is logical as they are glasses of the same type, sodalime glass. Similarly, the compositions of microflat glass (Table 8) and window glass (Table 1) are also quite similar, the microflat glass comes from building waste (building windows). Finally, it was found that the three mixed glasses (big, 12 mm and 8 mm) have a very similar composition, they are just processed to different particle sizes for their use as culled (see Figure 8).

The composition for glass-ceramic cooktops is within the Li_2O- Al_2O_3- SiO_2 system, with small amount of ZrO_2/TiO_2 as nucleating agents [2].

Table 7 Chemical analysis of container glasses.

Components	White glass		Amber glass		Green beer glass		Blue glass		Green wine glass		Laboratory glass	
	wt.%	mol%	wt.%	mol%	wt.%	mol%	wt.%	mol%	wt.%	mol%	wt.%	mol%
SiO_2	73.00	73.21	72.50	73.02	71.90	72.49	71.50	72.02	72.50	72.76	78.00	79.33
CaO	11.90	12.79	10.60	11.44	11.00	11.88	11.30	12.20	11.30	12.15	2.71	2.95
Fe_2O_3	0.10	0.04	0.44	0.17	0.47	0.18	0.13	0.05	0.46	0.17	0.10	0.04
K_2O	0.78	0.50	0.85	0.55	0.95	0.61	1.21	0.78	0.89	0.57	0.66	0.43
MgO	0.58	0.87	1.03	1.55	0.91	1.37	0.86	1.29	1.30	1.94	1.22	1.85
Al_2O_3	1.96	1.16	2.26	1.34	2.05	1.22	1.90	1.13	1.87	1.11	2.22	1.33
Na_2O	11.50	11.18	12.10	11.81	12.30	12.02	12.40	12.11	11.50	11.19	6.70	6.61
TiO_2	0.08	0.06	0.08	0.06	0.07	0.05			0.06	0.05	0.02	0.02
Cr_2O_3	0.02	0.01	0.05	0.02	0.31	0.12			0.07	0.03	0.02	0.01
SO_3	0.24	0.18	0.05	0.04	0.06	0.05	0.20	0.15	0.03	0.02	0.07	0.05
P_2O_5	0.02	0.01	0.03	0.01	0.03	0.01			0.03	0.01	0.02	0.01
B_2O_3											8.40	7.37
CoO							0.04	0.03				
CuO							0.32	0.24				

Table 8 Chemical analysis for the glass from the recycling company.

Components	White		Mixed		Mixed Fine 8 mm		Mixed Fine 12 mm		Microflat	
	wt.%	mol%	wt.%	mol%	wt.%	mol%	wt.%	mol%	wt.%	mol%
SiO_2	73.40	73.30	72.60	72.84	72.80	72.94	73.00	73.12	71.70	70.60
CaO	11.70	12.52	10.80	11.61	10.90	11.70	10.60	11.38	9.13	9.63
Fe_2O_3	0.10	0.04	0.27	0.10	0.29	0.11	0.33	0.12	0.20	0.07
K_2O	0.66	0.42	0.88	0.56	0.80	0.51	0.78	0.50	0.36	0.23
MgO	0.79	1.18	1.38	2.06	1.27	1.90	1.55	2.31	4.32	6.34
Al_2O_3	1.41	0.83	1.85	1.09	1.76	1.04	1.85	1.09	0.98	0.57
Na_2O	11.90	11.52	11.90	11.57	12.00	11.66	11.70	11.36	12.90	12.31
TiO_2	0.05	0.04	0.07	0.05	0.06	0.05	0.07	0.05	0.07	0.05
Cr_2O_3	0.02	0.01	0.10	0.04	0.09	0.04	0.07	0.03	0.02	0.01
SO_3	0.20	0.15	0.08	0.06	0.08	0.06	0.05	0.04	0.25	0.18

Funded by
the European Union

1.2.2 Dilatometry

Similarly as for commercial glasses, the thermal expansion coefficient, T_g and T_d have been determined for container glasses (white, amber, different green and blue). Figure 9 and Table 9 show both the dilatometric curves and the obtained results. As it can be seen, the thermal properties are very similar, where the T_g is around 560 °C and the thermal expansion coefficient is around 8- 8.5·10^{-6} K^{-1}. The small differences between the values may be due to the presence of different traces that give the characteristic colour to each container.

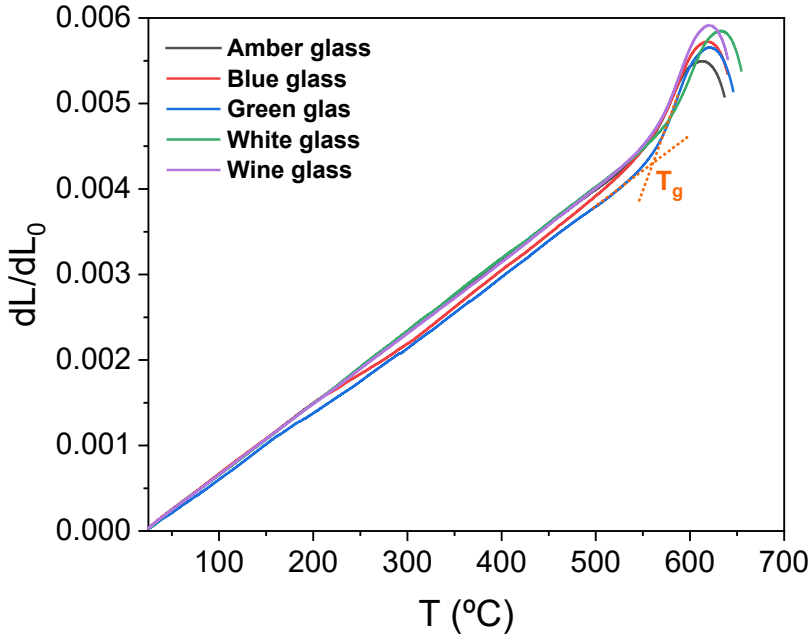

Figure 9 Dilatometric curves for the container glasses (amber, blue, green beer, white and green wine colours).

Table 9 Values of α, T_g and T_d for the different samples.

Glass sample	$\alpha^{(100-500\ °C)}$·10^{-6} (K^{-1})	T_g (°C)	T_d (°C)
Amber	8.4	559	612
Blue	8.0	559	619
Green beer	8.0	560	621
White	8.5	573	633
Green Wine	8.3	560	621

Finally, the same study was carried out for the glass-ceramic cooktop panel (Figure 10). Unlike the cases shown above, here it can be seen that the coefficient of thermal expansion is very low as expected for this type of material which makes it very resistant versus thermal changes.

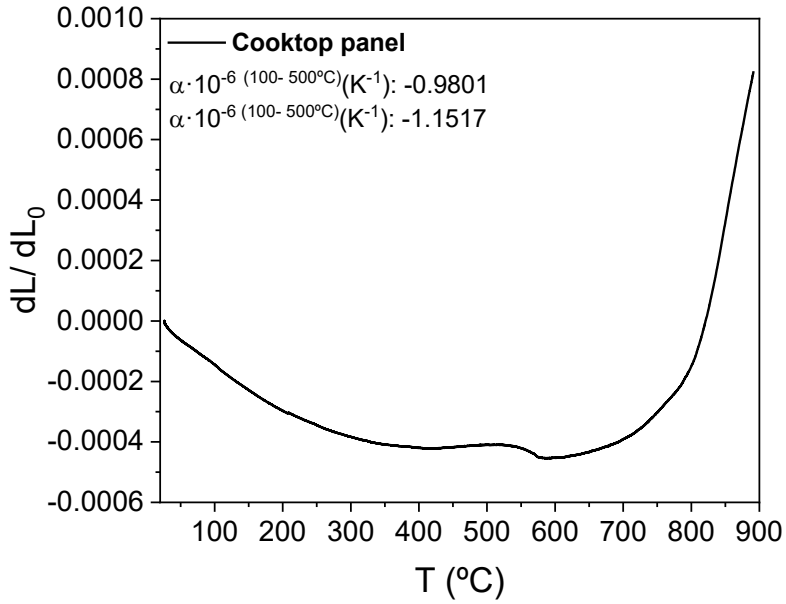

Figure 10 Dilatometric curve for cooktop panel glass-ceramic

1.2.3 Hot- stage microscopy (HSM)

HSM curves have been examined for the container glasses (Figure 11). The results obtained using this technique provide information on the viscosity reference points. The graph displays two temperatures: the temperature of first sintering (TFS) and the temperature of maximum sintering (TMS). Table 10 presents the results obtained for the three glasses.

Table 10 Viscosity fixed point temperatures.

Glass sample	TFS ± 10°C ($10^{9.1}$ dPa·s)	TMS ± 10°C ($10^{7.8}$ dPa·s)	Softening point ± 10 °C ($10^{6.3}$ dPa·s)	Sphere ± 10 °C ($10^{5.4}$ dPa·s)	Half- ball ± 10 °C ($10^{4.1}$ dPa·s)	Fluence ± 10 °C ($10^{3.4}$ dPa·s)
Amber	638	707	761	833	1030	1156
Blue	637	706	781	823	1034	1166
Green beer	643	718	783	828	1026	1115
White	641	717	779	831	1057	1152
Green Wine	637	713	732	838	1054	1167

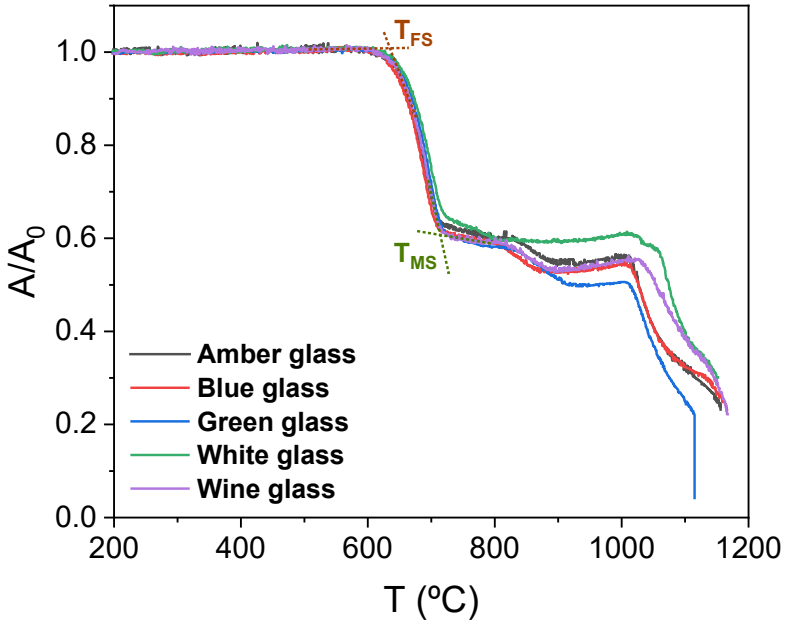

Figure 11 Hot- stage microscopy curves for container glasses.

Table 11 presents the fitting parameters derived from the Vogel-Fulcher-Tammann equation (VTF, eq. 1), where viscosity is plotted against temperature. The data for T_g, corresponding to log(η) = 13.3 dPa·s, have also been included. Figure 12 shows the viscosity-temperature curves for container glasses.

From the fitting, the parameters A, B, and T_0 of the equation are obtained. As observed, the viscosity of these glasses is quite similar (Figure 12) due to their very similar compositions.

Table 11 Parameters for fitting the equations of the viscosity-temperature curves.

Parameters	A	B	T_0
Amber glass	0.447	2338.2	372.5
Blue glass	0.464	2358.4	370.4
Green glass	0.278	2900.8	340.9
White glass	0.784	2064.9	402.9
Wine glass	0.887	2021.5	393.0

Funded by
the European Union

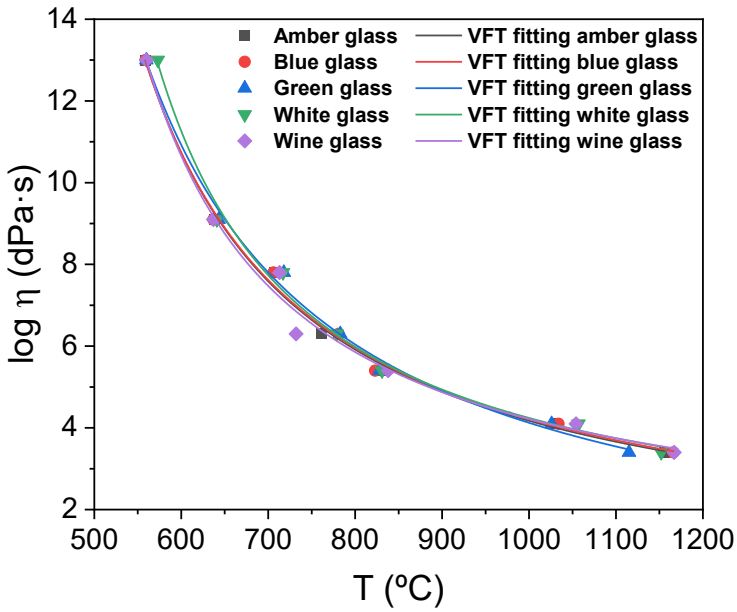

Figure 12 Viscosity-temperature curves for container glasses.

The same procedure was carried out for glass from the cullet- glass waste management company. The fixed points obtained by HSM (Table 12) have been used to plot the viscosity-temperature curves by means of the VTF fit.

Table 12 Viscosity fixed point temperatures.

Glass sample	TFS ± 10°C ($10^{9.1}$ dPa·s)	TMS ± 10°C ($10^{7.8}$ dPa·s)	Softening point ± 10 °C ($10^{6.3}$ dPa·s)	Sphere ± 10 °C ($10^{5.4}$ dPa·s)	Half- ball ± 10 °C ($10^{4.1}$ dPa·s)	Fluence ± 10 °C ($10^{3.4}$ dPa·s)
White	647	722	789	844	1044	1141
Mixed	640	715	792	830	1029	1133
Microflat	633	708	773	824	1018	1138

Table 13 provides the fitting parameters obtained from the VFT equation (Eq 1), where viscosity is plotted as a function of temperature. The data for T_g, which corresponds to log(η) = 13.3 dPa·s, are also included. Figure 13 illustrates the viscosity-temperature curves for container glasses.

From the fitting, the parameters A, B, and T_0 of the equation are obtained. As observed, the viscosity of these glasses is quite similar (Figure 10) due to their very similar compositions, although it can be noted that the viscosity increases in the following order: Fine< white< microflat. For comparison, the viscosity-temperature curve obtained for window glass has been included. These glasses have a very similar viscosity, which is to be expected as they are all sodalime glasses.

Table 13 Parameters for fitting the equations of the viscosity-temperature curves.

Parameters	A	B	T_0
White	-0.740	3542.6	290.7
Mixed	-0.514	3272.8	296.6
Microflat	-0.969	3771.2	269.4

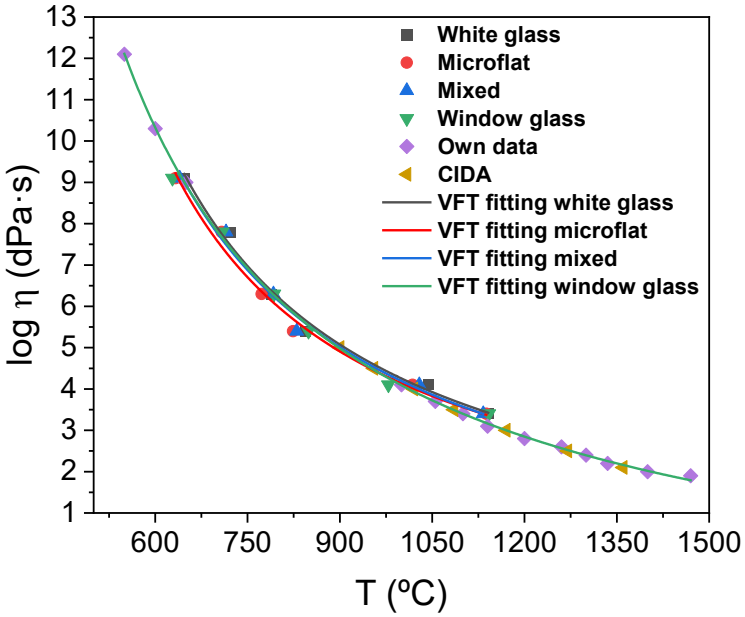

Figure 13 Viscosity-temperature curves for container glasses.

Finally, the same characterisation was carried out for the glass-ceramic material. Figure 14a) shows the HSM curve indicating flow temperatures higher than 1350ºC. Figure 14b) shows the viscosity-temperature curve for this material. As before, the corresponding VTF fitting has been performed, obtaining the parameters A, B, T_0; -14.42446, 12053.79137, 683.5262 °C respectively. Comparing with the parameters obtained for the other materials, it can be observed that the glass-ceramic is the most viscous.

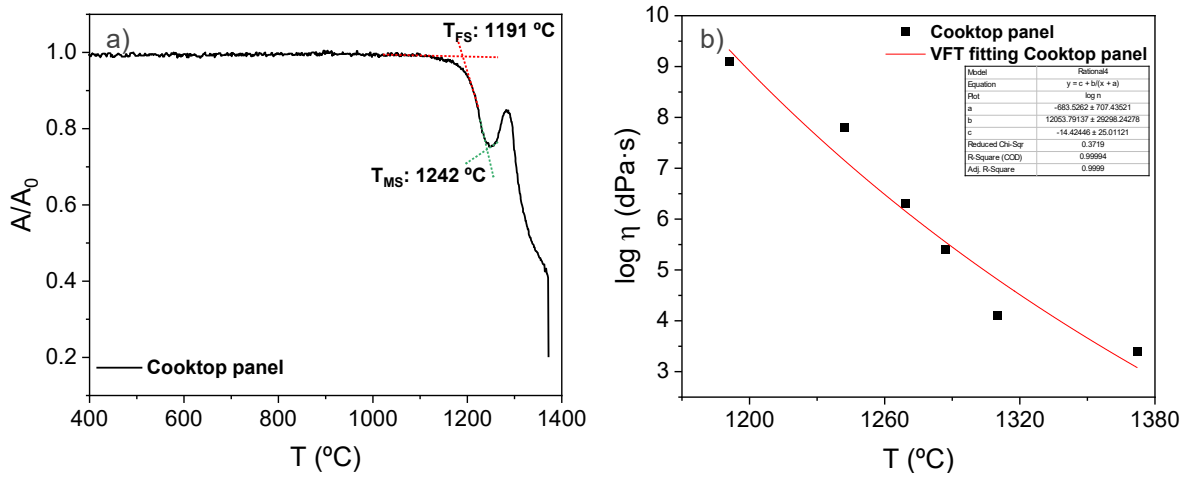

Figure 14 a) HSM curves and b) viscosity-temperature curves for the glass-ceramic cooktop.

The X-ray diffraction study was also carried out for this sample. Figure 15 shows the diffraction patterns obtained for cooktop panel powder (x< 20 µm). As it can be seen, the pattern corresponds to the lithium alumino-silicate with hexagonal symmetry ($Li_xAl_xSi_{1-x}O_2$, JCPDS 040- 0073). The crystal size has also been calculated using the Scherrer equation (Eq. 2) giving a value of 33 nm for 2θ≈ 25.7°.

$$\phi = \frac{0.94 \cdot \lambda}{cos\theta \cdot \sqrt{B_m^2 - B_i^2}} \qquad \text{Eq. 2}$$

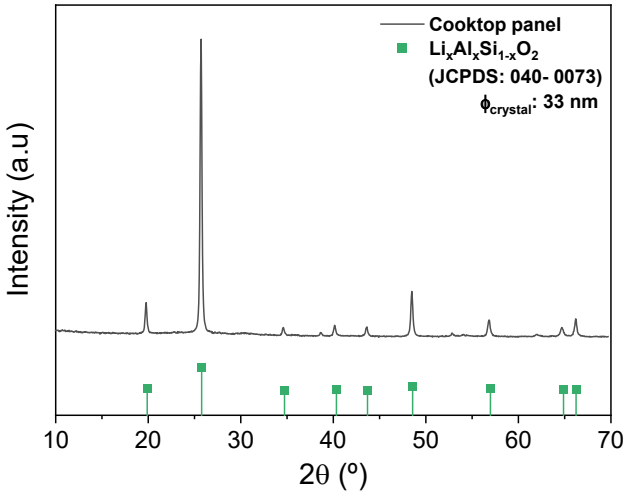

Figure 15 Diffraction pattern obtained for the cooktop panel.

1.2.4 Particle size

As mentioned above, these glasses need to be processed to obtain 200 g fractions with a particle size of 100-300 µm. For this purpose, they were first cleaned to remove possible residues, and then ground and sieved to the size of interest.

As an example, the corresponding particle size distribution for microphase glass is shown in Figure 16, while Table 14 shows the particle size values at different sample percentages. As can be seen, the particle size is below 400 µm while the average size (Dv(50)) is close to 200 µm for all bottle and container glasses. For the microflat (sample without previous milling) the size is 200 µm while the average is around 100 µm.

Table 14 Particle size values at different sample percentages.

Sample	Amber glass	Blue glass	Green glass	Lab glass	GC-Fagor	White glass	Window glass	Wine glass	Microflat glass
Dv(10) (µm)	139	44.9	101	111	73.3	127	114	112	68
Dv(50) (µm)	261	215	202	231	190	248	231	221	137
Dv(100) (µm)	421	397	362	400	343	409	400	390	233

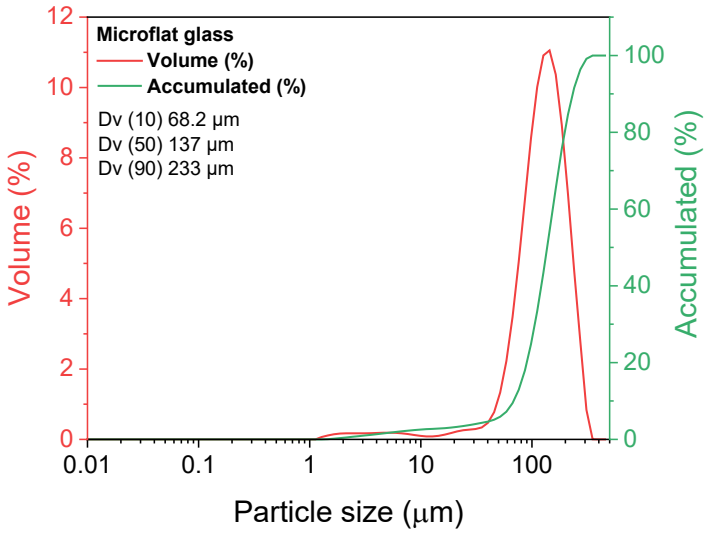

Figure 16 Particle size distribution of glass powder microflat glass.

Fractions of 200 g of all glass materials have been prepared in the particle size 300-100 µm for laser processing and send it to Vigo University. At the ICV-CSIC, glass wastes and mixtures of them will be melted using conventional gas furnace and electric furnaces in order to compare the final pieces obtained with those processed by laser melting and morphing.

2 Relevance of viscosity- temperature curves

2.1 Establishment of the working range for the laser melting and morphing process

Figure 17 highlights the importance of understanding viscosity-temperature curves, particularly in defining the working range for processes involving laser melting and morphing of materials like glass. These curves are crucial in determining the precise temperatures at which glass can be effectively processed using lasers. The figure shows the viscosity values which are relevant in glass melting and processing of glass containers (pressing, blowing, molding, etc..). The optimum viscosity-temperature range must be determined when using glass morphing by laser to give shape to a product in absence of any mold and not compromise its structural integrity. By establishing this working range, manufacturers can optimize laser processes.

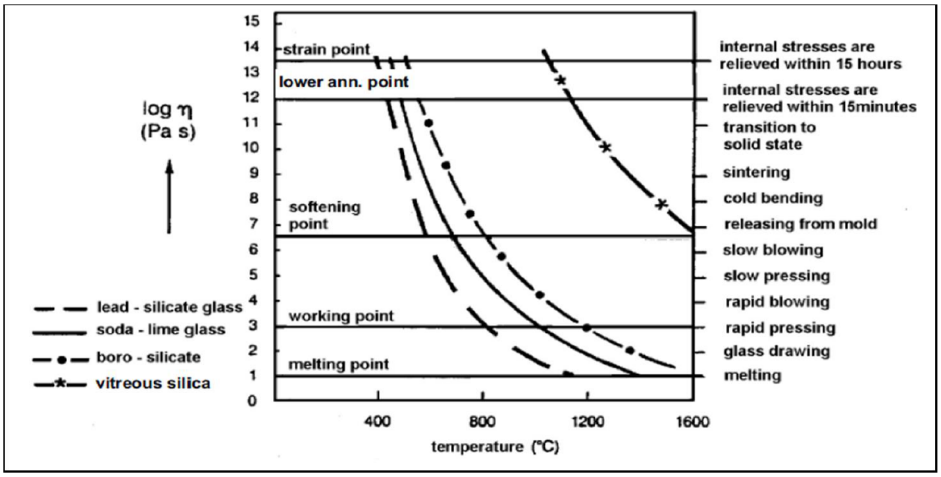

Figure 17 Typical viscosity-temperature curves for glasses of different systems. "Strong glass" (gradual variation of viscosity with temperature). "Fragile glass" (fast variation of viscosity with temperature).

2.2 Establishment of the annealing curves for the different types of glasses. Corning programme

The establishment of annealing curves for the different types of glass which involves determining the optimum thermal cycles necessary to relieve internal stresses without causing deformation or other undesirable effects is also another key issue. Annealing is a process in which glass is slowly cooled from a high temperature to release internal stresses caused by uneven cooling. The annealing point is the temperature at which the internal stresses in the glass are most effectively relieved, and different types of glass, depending on their composition, have different annealing points and require different annealing schedules.

Each type of glass has specific properties that determine its annealing curve. For example, sodalime glass, common in windows and bottles, typically has an annealing point of around 550 °C. Borosilicate glass, used in laboratory equipment and cookware, has a higher annealing point, around 560 °C, due to its lower coefficient of thermal expansion. Aluminosilicate glass, known for its high strength and durability, such as that used in smartphone screens, has annealing points that vary according to its specific composition.

The Corning method, widely used in the glass industry, is an empirical approach to calculate the annealing curve of glass, which is essential for removing internal stresses from the material and ensuring its mechanical and optical stability. This method is based on the relationship between glass viscosity

and temperature, described through viscosity-temperature curves. These curves allow predicting how the viscosity of the glass changes during the cooling process. These curves must also be adapted to pieces after the morphing process by laser.

Viscosity is a critical factor because it determines how easily the glass can be deformed. At high temperatures, viscosity is low, which means that the glass is more fluid and therefore more capable of relieving stresses. As the temperature decreases, the viscosity increases, and the glass becomes stiffer. Viscosity-temperature curves provide a way to model this behaviour, allowing engineers to design an annealing cycle that ensures controlled cooling.

The Corning method uses these curves to determine the optimum temperatures and dwell times for each phase of annealing. The objective is to keep the glass within a viscosity range where internal stresses can be relaxed without deformation of the material.

In the case of the use of this GLM methodology, after the melting and shaping of the glass part it is necessary to perform a slow cooling which will be the annealing of the glass part.

3 Conclusion

This research focuses on the characterisation and potential reuse of both commercial and recycled glass and the conditioning of glass powders that can be fed in the laser morphing machine in order to obtain a new final glass product. The chemical composition and thermal properties of these glasses were examined extensively, revealing significant variations, particularly in the concentrations of key elements such as SiO_2, B_2O_3 and Al_2O_3. These differences are critical, as they directly influence the viscosity and other thermal properties of the glass, essential factors in determining its suitability for various applications.

Through the analysis of viscosity-temperature curves, the study provided a deeper understanding of how the specific chemical composition of glass affects its behaviour during heating processes. For instance, the presence of Al_2O_3 was found to impact the viscosity of the glass at lower temperatures, whereas components like Na_2O influenced its behaviour across a broader temperature range. These insights are crucial for tailoring the glass properties to specific industrial processes, such as Glass Laser Morphing (GLM).

Despite the observed differences in composition and thermal properties, the sodaline glasses for containers and the float glass for windows have been found to exhibit similar properties. This is particularly relevant for sustainable manufacturing using the GLM method as it will allow optimisation of both melting and annealing temperatures.

All the physico-chemical data of the precursor glasses are also relevant for the mathematical modelling of the laser melting and morphing process.

Finally, 200 g of the different glasses with a particle size of 100-300 microns have been prepared for their corresponding laser processing and delivered to Vigo University. These glasses are:

- Window glass
- Covid vaccine
- Duran® glass
- White glass
- Blue glass
- Amber glass
- Green glass

- Wine glass
- Laboratory glass
- Microflat glass
- Cooktop Fagor
- White glass (Daniel Rosas's wastes)
- Mixed glass (Daniel Rosas's wastes)

At the ICV-CSIC, glass wastes and mixtures of them will be melted using conventional gas furnace and electric furnaces in order to compare the final pieces obtained with those processed by laser melting and morphing. Additionally other types of glass wastes will be collected for continuing investigation.

References

[1] Products | SCHOTT Pharma, (n.d.). https://www.schott-pharma.com/en/products (accessed September 9, 2024).

[2] SCHOTT AG, Glass ceramic substrate made of a transparent, colored LAS glass- ceramic and method for producing it, 2014.

Annex

a) Annex 1

Table 15 which includes the viscosity set points for Duran and window glass given by the commercial companies.

Table 15 Fixed viscosity points for Duran and window glass including the data given by the commercial companies

Duran® glass		Window glass					
		Fixed points		ICV-CSIC data		CIDA (Saint-gobain)	
T (°C)	Logη (dPa·s)	T (°C)	Logη (dPa·s)	T (°C)	Logη (dPa·s)	T (°C)	Logη (dPa·s)
560	13	628	9.1	550	12.1	900	5
689	9.1	709	7.8	600	10.3	955	4.5
801	7.8	793	6.3	650	9	1020	4
860	7.6	849	5.4	1000	4.1	1085	3.5
870	6.3	979	4.1	1055	3.7	1170	3
1140	5.4	1142	3.4	1100	3.4	1270	2.5
1235	4.1			1140	3.1	1360	2.1
1269	4			1200	2.8		
1431	3.4			1260	2.6		
				1300	2.4		
				1335	2.2		
				1400	2		
				1470	1.9		

b) Annex 2

Table 16 temperature and viscosity data used to represent the viscosity-temperature curves for PGW glass powder and microspheres.

Table 16 Viscosity and temperature values estimated for PGW.

		Glass powder	Glass microsphere	Δ(GM-GP)
	$Log_{10}η$ (dPa·s)	T (°C)	T (°C)	T (°C)
Melting point	2	1625.2	1738.2	113
	2.5	1465.5	1571	105.5
	3	1337.6	1435.7	98.1
W. p. (press, blow)	4	1145.6	1230.3	84.7
	5	1008.4	1081.6	73.2
	6	905.3	969	63.7
	7	825.2	880.8	55.6
Littleton softening point	7.6	785.1	836.5	51.4

	8	761	809.9	48.9
	9	708.5	751.5	43
	10	664.7	702.8	38.1
	11	627.6	661.3	33.7
	11.5	611.2	642.9	31.7
T_g area	12	595.9	625.7	29.8
	13	568.3	594.8	26.5
	13.3	560.8	586.3	25.5
	14	544.2	567.7	23.5
	14.5	533.2	555.3	22.1

Funded by
the European Union